

## Diamond-Anvil Cell Observations of a New Methane Hydrate Phase in the 100-MPa Pressure Range

I-Ming Chou,<sup>†</sup> Anurag Sharma,<sup>‡</sup> Robert C. Burruss,<sup>§</sup> Russell J. Hemley,<sup>‡</sup>  
Alexander F. Goncharov,<sup>‡</sup> Laura A. Stern,<sup>||</sup> and Stephen H. Kirby<sup>||</sup>

954 National Center, U.S. Geological Survey, Reston, Virginia 20192, Geophysical Laboratory and Center for High Pressure Research, Carnegie Institution of Washington, 5251 Broad Branch Rd., N.W., Washington, D.C. 20015, 956 National Center, U.S. Geological Survey, Reston, Virginia 20192, and MS/977 U.S. Geological Survey, Menlo Park, California 94025

Received: July 31, 2000; In Final Form: January 9, 2001

A new high-pressure phase of methane hydrate has been identified based on its high optical relief, distinct pressure–temperature phase relations, and Raman spectra. In-situ optical observations were made in a hydrothermal diamond-anvil cell at temperatures between  $-40^{\circ}$  and  $60^{\circ}$  C and at pressures up to 900 MPa. Two new invariant points were located at  $-8.7^{\circ}$  C and 99 MPa for the assemblage consisting of the new phase, structure I methane hydrate, ice Ih, and water, and at  $35.3^{\circ}$  C and 137 MPa for the new phase–structure I methane hydrate–water–methane vapor. Existence of the new phase is critical for understanding the phase relations among the hydrates at low to moderate pressures, and may also have important implications for understanding the hydrogen bonding in H<sub>2</sub>O and the behavior of water in the planetary bodies, such as Europa, of the outer solar system.

Methane hydrate is a crystalline nonstoichiometric compound composed of water and methane. It commonly occurs naturally along the continental shelves and in permafrost areas<sup>1</sup> and has been the subject of increasing interest throughout the world because of its environmental, energy resource, and planetary significance. Methane hydrate is a potential energy source due to its abundance in nature,<sup>2</sup> it is an agent for global warming,<sup>3</sup> its decomposition may cause landslides and instability of continental shelves, and it may plug commercial gas pipelines. Studies of this material may also enhance our understanding of the nature of hydrogen bonding in H<sub>2</sub>O, and the behavior of water in the planetary bodies in the outer solar system.<sup>4</sup> The behavior of methane hydrate as a function of pressure and temperature is critical for each of these issues, and therefore, studies of its physicochemical properties have attracted increasing attention. Through hydrogen bonding, the water molecules are connected to each other to form two kinds of clathrate cages; the smaller one is a pentagonal dodecahedron (denoted by  $5^{12}$  for 12 pentagonal faces), and the larger one is a tetrakaidecahedron ( $5^{12}6^2$  for 12 pentagonal with 2 additional hexagonal faces). Each cage structure is stabilized by inserting a methane molecule, and a cubic unit cell of methane hydrate ( $a = 12 \text{ \AA}$ ; known as structure I methane hydrate) contains six  $5^{12}6^2$  and two  $5^{12}$  cages, with an ideal H<sub>2</sub>O/CH<sub>4</sub> ratio of 46/8 (or a hydration number of 5.75).<sup>1</sup> In the presence of other components such as ethane, propane, or methylcyclohexane, methane can occur in the cages of structure II and structure H hydrates. The cubic unit cell of structure II contains sixteen  $5^{12}$  and eight  $5^{12}6^4$  cages, with a total of 136 H<sub>2</sub>O, and the rhombohedral unit cell

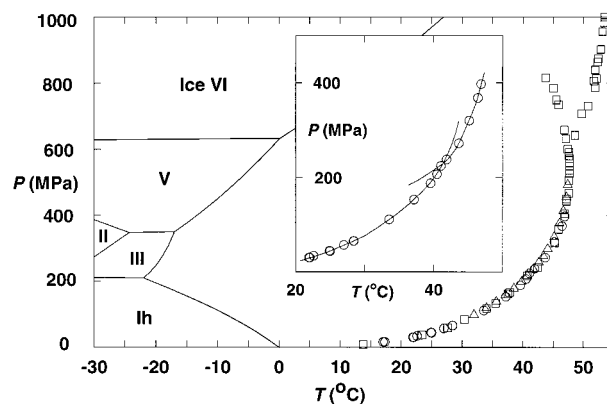


**Figure 1.** Summary of previous experimental data for the univariant  $P$ – $T$  relations of the assemblage methane hydrate–water–methane vapor; data were taken from Marshall et al.<sup>8</sup> (circles), Dyadin et al.<sup>7</sup> (squares), and Nakano et al.<sup>9</sup> (triangles). The boundaries for the stable ice phases and their melting curves (solid lines) are from Haselton et al.<sup>17</sup> The insert shows the kink of the  $P$ – $T$  curve reported by Marshall et al.<sup>8</sup> near  $41^{\circ}$  C. Data above 1000 MPa<sup>7</sup> were not shown.

of structure H contains three  $5^{12}$ , two  $4^35^66^3$ , and one  $5^{12}6^8$  cages, with a total of 34 H<sub>2</sub>O.<sup>1,5,6</sup>

For pure methane hydrate at high pressure (approximately 620 MPa), a distinct transition to an additional, unidentified phase occurs to structure I methane hydrate as shown in Figure 1.<sup>7</sup> The earliest high-pressure phase equilibrium study<sup>8</sup> documented a small kink in the solid–liquid–vapor univariant pressure–temperature ( $P$ – $T$ ) curve for methane hydrate at intermediate pressures (about 223 MPa,  $41^{\circ}$  C) as shown in Figure 1. Although ignored in the original work, this kink suggests the presence of a phase transition in the methane hydrate system. However, subsequent work<sup>9,10</sup> did not show any evidence for such a phase transition in this pressure range

<sup>†</sup> 954 National Center, U.S. Geological Survey, Reston, Virginia.

<sup>‡</sup> Geophysical Laboratory and Center for High Pressure Research, Carnegie Institution of Washington.

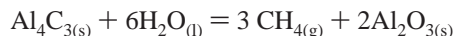
<sup>§</sup> 956 National Center, U.S. Geological Survey, Reston, Virginia.

<sup>||</sup> MS/977 U.S. Geological Survey, Menlo Park, California.

(Figure 1). In this study, we report the direct observation in this pressure range of a new methane hydrate phase that can explain the previously reported discontinuity in the univariant  $P$ - $T$  curve.

To understand the high-pressure phase behavior of methane hydrate, in-situ observations were made in a hydrothermal diamond anvil cell<sup>11</sup> under a microscope, and the presence of a new high-pressure phase was documented by Raman spectroscopy. Raman spectroscopy has been used to identify the type of clathrate hydrate cage that contains methane,<sup>6,12</sup> uniquely identifying the 5<sup>12</sup> and 5<sup>12</sup>6<sup>2</sup> cages of structure I, the 5<sup>12</sup> and 5<sup>12</sup>6<sup>4</sup> cages of structure II, and the 5<sup>12</sup> and 4<sup>3</sup>5<sup>6</sup>6<sup>3</sup> cages of structure H. Methane has not been documented in the 5<sup>12</sup>6<sup>8</sup> cage of structure H by any method. Our results show that several phase transitions can be observed, and some of these phase transitions project to lower pressure and temperature conditions, suggesting that they may impact the stability of gas hydrate phases in the deep ocean and in high-pressure engineering applications.

Diamond cell observations were made between  $-40^\circ$  and  $60^\circ$  °C, and at pressures up to 900 MPa. To prepare samples, synthetic methane hydrate<sup>13</sup> was loaded in the sample chamber of the cell (a hole of about 500  $\mu\text{m}$  diameter in a 250  $\mu\text{m}$  thick stainless steel gasket sandwiched between two diamond anvil faces). After the sample chamber is sealed, the total mass of the sample remains constant. The bulk density (and sample pressure) is then adjusted by changing the volume of the sample chamber, achieved by adjusting the distance between the two diamond-anvil faces. Once the volume of the sample chamber is fixed, the sample remains under isochoric conditions.<sup>14</sup> Thermal expansion of various parts of the cell, within the small temperature range of this study, has a negligible effect on the sample volume. Occasionally, samples were prepared by sealing  $\text{Al}_4\text{C}_3$  and distilled water in the sample chamber, and  $\text{CH}_4$  was generated at temperatures above 200 °C by the reaction



where s, l, and g represent solid, liquid, and gas, respectively. Even though there are no noticeable differences between results obtained in these two different loading methods, the  $\text{Al}_2\text{O}_3$  powder generated in the reaction commonly hindered optical observations.

The pressure of the sample chamber was estimated from the temperature at which the hydrate started to decompose with the formation of methane vapor (see Figure 1 for the  $P$ - $T$  relations). This  $P$ - $T$  point defines the density of the coexisting water. The sample pressure at lower temperatures, before the formation of ice, can be calculated from the isochore of  $\text{H}_2\text{O}$  of this particular density.<sup>15</sup> The bulk sample density was then increased by compressing the gasket with the two diamond anvils, and the new sample pressure, resulting from the reduction of sample volume, was determined in the same fashion. Typically, the sample pressure was high enough that methane hydrate was stable in the presence of water at room temperature.

The growth of both the new high-pressure phase and structure I crystals during a cooling cycle is shown in Figure 2. Crystals of the new phase (crystals A, B, C, and D in Figure 2) have a higher optical relief, and a distinctly different Raman spectrum from that of structure I phase (Figure 3a). The pressures given in Figure 2 (a) to (d) were calculated from the data of Nakano et al.<sup>9</sup> for the assemblage structure I methane hydrate-water-methane vapor and should be slightly higher than the actual pressures because of the presence of the new phase instead of structure I phase (see Figure 4). The pressure given in (e) was

calculated from the equation of state of water<sup>15</sup> for a density of 1046.8  $\text{kg}/\text{m}^3$ . In-situ Raman spectra were measured with Ar-ion lasers (514.5 nm excitation wavelength). The spectra were typically collected for 1500 s using an Andor CCD detector cooled to  $-90^\circ$  °C mounted on a TRIAX 550 spectrometer with a 1500 grooves/mm grating. The  $\text{CH}_4$   $\nu_1$  band for the new phase is a doublet with peaks at 2904 and 2910  $\text{cm}^{-1}$ , with a peak height ratio of about 1:3. In comparison, the  $\nu_1$  band for structure I phase is a doublet at 2904 and 2915  $\text{cm}^{-1}$ , with an intensity ratio of 3:1, reflecting the number of large cages in a unit cell of this structure is three times of that for small cages.<sup>12</sup> Raman spectra for the new phase suggest that the number of small cages in the structure is greater than the number of large cages, analogous to the structure II and structure H hydrates. However, the peak position for  $\text{CH}_4$  in the small cages in the new phase is at 2910  $\text{cm}^{-1}$ , which is different from those of structure II (2913.7  $\text{cm}^{-1}$  for deuterated tetrahydrofuran containing phase,<sup>12</sup> and 2914.8  $\text{cm}^{-1}$  for the phase containing 0.27 mole fraction of ethane.<sup>18</sup>) and structure H (2912.8  $\text{cm}^{-1}$  for deuterated methylcyclohexane containing phase.<sup>12</sup>)

In some of our experiments, structure I methane hydrate was found to metastably exist at higher pressures. Figure 3b shows the Raman spectra of structure I methane hydrate at 25 °C and at pressures of 125, 649, and 880 MPa. The shift of the methane peak for the small cavity from 2915  $\text{cm}^{-1}$  to about 2921  $\text{cm}^{-1}$ , as pressure increases from 125 to 880 MPa, is in agreement with the shift reported by Nakano et al.,<sup>9</sup> except the effect of pressure on the peak position is not as strong. Apparently, the new high-pressure phase was not formed (or observed) in the experiments of Nakano et al.<sup>9</sup> and Hirai et al.<sup>10</sup>

Phase relations in the system  $\text{CH}_4$ - $\text{H}_2\text{O}$  were determined by optical observations of the sample in the diamond cell during cooling and heating. In the presence of the new phase, structure I methane hydrate and water, ice Ih was formed during further cooling of the sample to about  $-40^\circ$  °C. The invariant point, for the assemblage of the new phase-structure I methane hydrate-ice Ih-water (point B in Figure 4), was located by the melting temperature of ice Ih at  $-8.7(\pm 0.3)^\circ$  °C during warming of the sample.<sup>16</sup> In theory, in the presence of the new high-pressure phase and structure I methane hydrate, ice Ih melts at an invariant point (fixed  $P$  and  $T$ ). However, in the presence of the new phase and structure I methane hydrate, ice Ih was observed to melt over a range of  $P$ - $T$  conditions, indicating nonequilibrium conditions. Equilibrium is not expected to be achieved during our ice melting experiment under a heating rate of about 0.02 °C/s. Here, the invariant point was defined by the temperature at which the last crystal of ice Ih melts. On the basis of the equation of state of  $\text{H}_2\text{O}$ ,<sup>16</sup> the pressure of this invariant point is 99 MPa, and the density of water at this point is 1046.8  $\text{kg}/\text{m}^3$ .

On further warming, the sample followed the  $P$ - $T$  path shown as line BC in Figure 4, where the line ended at the invariant point C for the assemblage of the new phase-structure I methane hydrate-water-methane vapor. This invariant point was defined during warming by the temperature at which the first methane bubble appeared ( $35.3 \pm 0.5^\circ$  °C). Note that this observation is in agreement with the temperature at which the last methane vapor bubble almost disappeared at 35.9 °C during a cooling experiment (Figure 2d). The pressure of this invariant point, defined by the water density of 1046.8  $\text{kg}/\text{m}^3$  at 35.3 °C, is 136.7 MPa.<sup>15</sup> This pressure is very close to the values of 131.0 and 134.6 MPa, interpolated from the data of Marshall et al.<sup>8</sup> and Nakano et al.,<sup>9</sup> respectively, for the assemblage structure I methane hydrate-water-methane vapor at 35.3 °C.

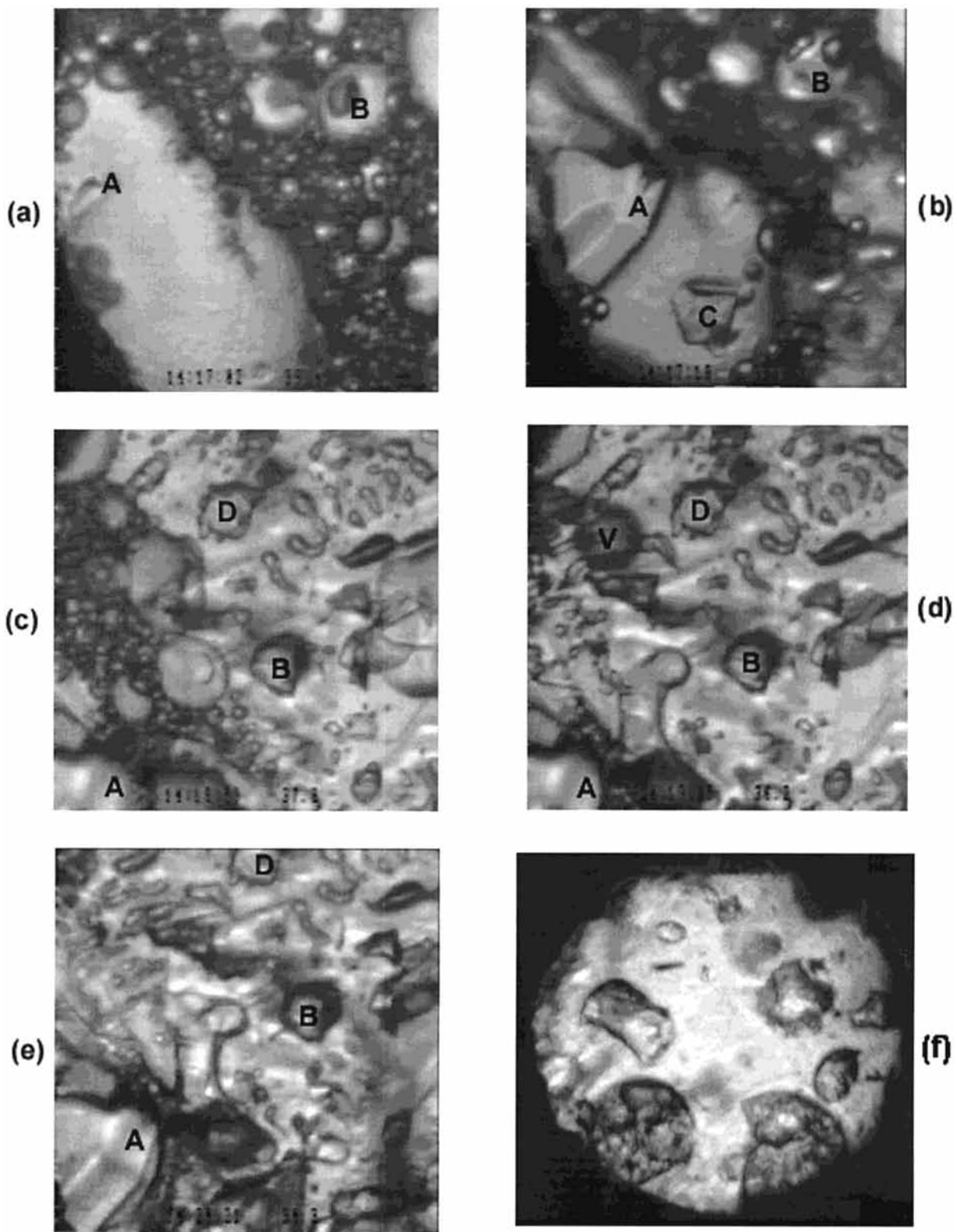


**Figure 2.** Images (a to e) of a sample during a cooling cycle, and image of another sample (f) showing the optical relief of the new phase crystals. (a) The initial crystallization of the new methane hydrate phase (crystal A) in coexisting water and methane vapor at 39.2 °C and 190 MPa. Crystal B is the only crystal of the new phase, which survived at 41 °C and 223 MPa before cooling started. (b) The growth of the new phase (crystal A) and the euhedral growth of the new phase (crystal C) at 38.5 °C and 178 MPa in the presence of water and methane vapor. (c) The euhedral growth of the new phase (crystals B and D) in the presence of water and methane vapor (see bubbles at the center left) at 37.5 °C and 163 MPa. Crystal A appears at the lower left corner. (d) The new phase (crystals A, B, D), and the last vapor bubble (V) in water at 35.9 °C and 142 MPa. (e) The coexistence of the new phase (crystals A, B, D, and many other high-relief crystals), structure I methane hydrate crystals (low-relief background crystals), and water at 35.0 °C and 136 MPa. The field of view is about 0.3 mm, and the sample is about 0.25 mm thick. (f) In another sample, the new phase (high-relief crystals) coexists with structure I methane hydrate (background) and water at 25 °C and 125 MPa. The sample chamber is about 0.3 mm in diameter and 0.25 mm thick.

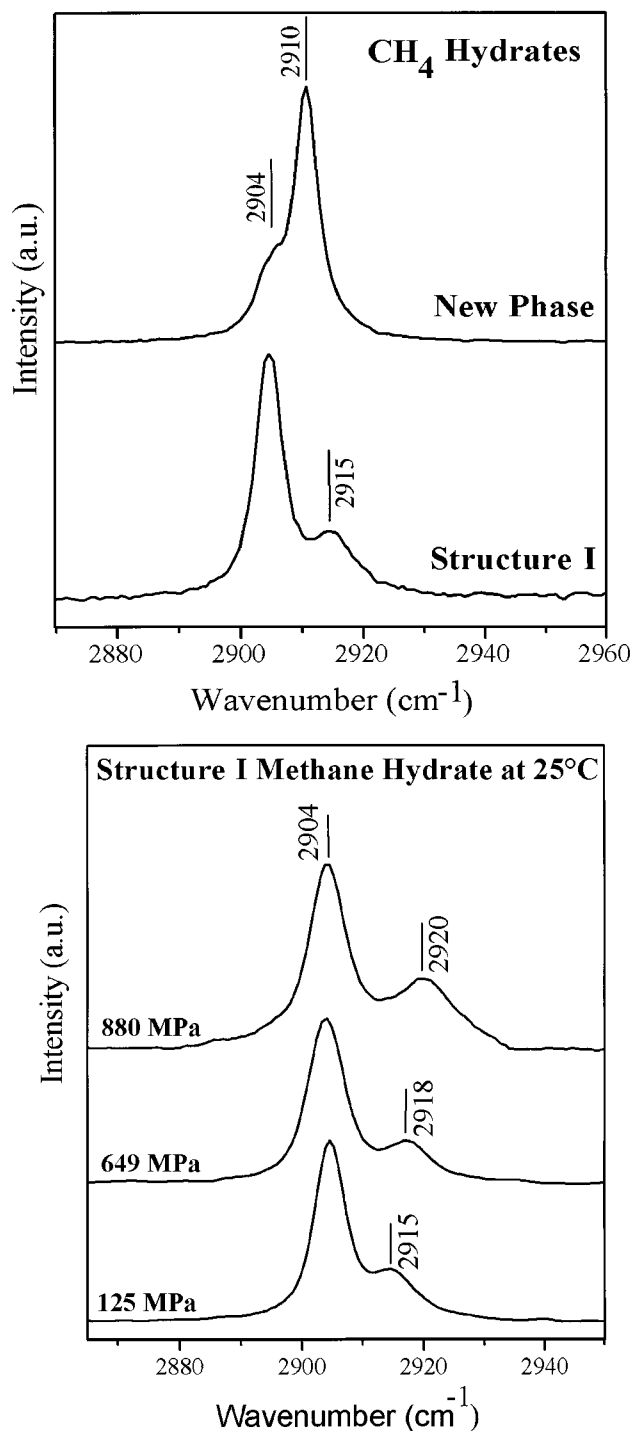


**Figure 3.** Raman spectra of (a; top) the new methane hydrate phase (high-relief crystals shown in Figure 2) and structure I methane hydrate (low-relief back ground crystals shown in Figure 2d) at 25 °C and 125 MPa; and (b; bottom) structure I methane hydrate at 25 °C and at pressures of 125, 649, and 880 MPa.

In all of these pressure calculations, the equation of state of pure water was used, under the assumption that the dissolution of methane in water has a negligible effect on its volumetric behavior.

In summary, a high-pressure form of methane hydrate was identified near 125 MPa at room temperature, based on its high optical relief, distinct pressure–temperature phase relations, and Raman spectra. Additionally, the crystals of the new phase do not show any birefringence under crossed polarizers, suggesting a cubic symmetry. Its stability phase relations are summarized

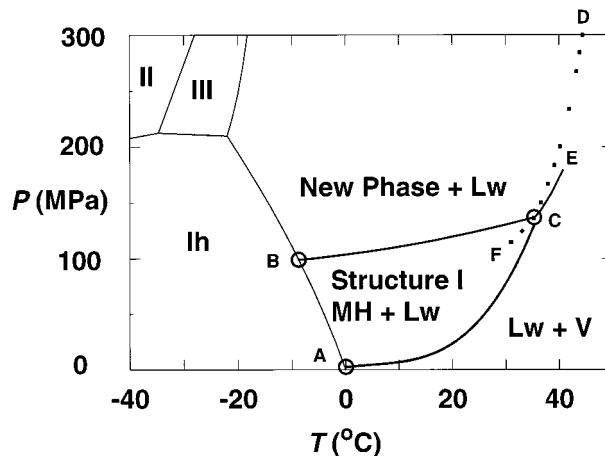


**Figure 4.** Phase relations for the system  $\text{CH}_4\text{-H}_2\text{O}$ . The three invariant points shown as open circles at A (1.2 MPa and 0 °C), B (99 MPa and -8.7 °C), and C (137 MPa and 35.3 °C) are for the assemblages of structure I methane hydrate (MH)–ice Ih–water–methane vapor, the new phase–structure I methane hydrate–ice Ih–water, and the new phase–structure I methane hydrate–water–methane vapor, respectively. The solid curve BC is the isochore of pure water having the density of 1046.8  $\text{kg/m}^3$ , which approximates the univariant curve for the assemblage of the new phase–structure I methane hydrate–water. The solid curve AC and the dotted line CD are, respectively, the stable and metastable univariant lines for the assemblage structure I methane hydrate–water–methane vapor. The schematic solid line CE and dotted line CF are, respectively, the stable and metastable univariant curves for the assemblage of the new phase–water–methane vapor. The univariant curve for the assemblage of the new phase–structure I methane hydrate–ice Ih, branches to the left of point B, is not shown. The phase boundaries between ice polymorphs and their melting curves are from Haselton et al.<sup>17</sup>

in Figure 4, including two new invariant points (points B and C) and one new univariant curve (line BC). The solid curve AC and the dotted line CD are, respectively, the stable and metastable univariant lines for the assemblage structure I methane hydrate–water–methane vapor. The dashed line CD is based on the experimental data of Nakano et al.<sup>9</sup> On the basis of a geometric approach after the method of Schreinemakers,<sup>19</sup> the stable univariant curve CE and metastable univariant curve CF for the assemblage of the new phase–water–methane vapor are shown schematically in Figure 4. With additional control of nucleation and crystallization, we were able to synthesize single crystals of the new phase at the pressures and temperatures indicated for its stability field. This confirms our findings regarding the stability fields for structure I methane hydrate and the new phase. Efforts are underway to examine the new phase using micro diffraction and synchrotron-x-radiation techniques. The stability range of the new phase indicates that it is the form of methane hydrate that would exist in the deep parts of marine sediments. Moreover, it could be present and constitute a carbon and water reservoir in icy satellites such as Europa or even perhaps within the Martian crust.

**Acknowledgment.** Work by I.M.C., L.A.S., and S.H.K. was partly supported by the Lawrence Livermore National Laboratory Gas Hydrates Program through its Laboratory Directed Research and Development Office. Work performed by A.S., A.F.G., and R.J.H. was supported by the NSF Center for High Pressure Research and the NASA Astrobiology Institute.

## References and Notes

- (1) Sloan, E. D., Jr. *Clathrate Hydrates of Natural Gases*, 2<sup>nd</sup> ed.; Marcel Dekker: New York, 1997.

- (2) Kvenvolden, K. A. *Chem. Geol.* **1998**, *71*, 41.
- (3) Kvenvolden, K. A. *Global Biogeochem. Cycles* **1988**, *2*, 221.
- (4) Anderson, J. D.; Lau, E. L.; Sjogren, W. L.; Schubert, G.; Moore, W. B. *Science* **1997**, *276*, 1236.
- (5) Dyadin, Y. A.; Bondaryuk, I. V.; Zhurko, F. V. In *Inclusion Compounds, Inorganic and Physical Aspects of Inclusion*; Atwood, J. L., Davies, J. E. D., MacNicol, D. D. Eds.; Oxford University Press: 1991, Vol. 5, pp 213–275.
- (6) Subramanian, S.; Ph. D. dissertation, Colorado School of Mines, 2000.
- (7) Dyadin, Y. A.; Aladko, E. Y.; Proceedings, 2nd International Conference on Natural Gas Hydrates, June 2–6, 1996, Toulouse, France, pp 67–70. Dyadin, Y. A.; Aladko, E. Y.; Larionov, E. G.; *Mendeleev Communications* **1997**, *1*, 34.
- (8) Marshall, D. R.; Saito, S.; Yashi, R. K.; *A. I. Ch. E. J.* **1964**, *10*, 202.
- (9) Nakano, S.; Moritoki, M.; Ohgaki, K.; *J. Chem. Eng. Data* **1999**, *44*, 254.
- (10) Hirai, H.; Kondo, T.; Hasegawa, M.; Yagi, T.; Yamamoto, Y.; Komai, T.; Nagashima, K.; Sakashita, M.; Fujihisa, H.; Aoki, K. *J. Phys. Chem. B* **2000**, *104*(7), 1429–1433.
- (11) Bassett, W. A.; Shen, A. H.; Bucknum, M.; Chou, I. M. *Rev. Sci. Instr.* **1993**, *64*, 2340.
- (12) Sum, A. K.; Burruss, R. C.; Sloan, E. D., Jr. *J. Phys. Chem. B* **1997**, *101*, 7371.
- (13) Stern, L. A.; Kirby, S. H.; Durham, W. B. *Science* **1996**, *273*, 1843.
- (14) Chou, I. M.; Blank, J. G.; Goncharov, A. F.; Mao, H. K.; Hemley, R. J. *Science* **1998**, *281*, 809.
- (15) Saul, A.; Wagner, W. *J. Phys. Chem. Ref. Data* **1989**, *18*, 1537.
- (16) Wagner, W.; Saul, A.; Prua, A. *J. Phys. Chem. Ref. Data* **1994**, *23*, 515.
- (17) Haselton, H. T., Jr.; Chou, I-Ming; Shen, A. H.; Bassett, W. A. *Am. Mineral.* **1995**, *80*, 1302.
- (18) Subramanian, S.; Kini, R. A.; Dec, S. F.; Sloan, E. D., Jr. *Chem. Eng. Sci.* **2000**, *55*, 1981.
- (19) Zen, E-An *U. S. Geological Survey Bulletin* **1966**, 1225.